CSIRO PUBLISHING
Soil Research, 2014, **52**, 140–154
http://dx.doi.org/10.1071/SR13179

Soil genesis on hypersaline tidal flats (*apicum* ecosystem) in a tropical semi-arid estuary (Ceará, Brazil)

A. G. B. M. Albuquerque[A], *T. O. Ferreira*[B,F], *G. N. Nóbrega*[B], *R. E. Romero*[A], *V. S. Souza Júnior*[C], *A. J. A. Meireles*[D], *and X. L. Otero*[E]

[A]Departamento de Ciências do Solo, Universidade Federal do Ceará, UFC, M.B.12168, Fortaleza, Ceará, Brazil.
[B]Departamento de Ciência do Solo, Escola Superior de Agricultura Luiz de Queiroz, Universidade de São Paulo, ESALQ/USP, Piracicaba, São Paulo, Brazil.
[C]Departamento de Agronomia, Universidade Federal Rural de Pernambuco, UFRPE, Recife – Pernambuco, Brazil.
[D]Departamento de Geografia, Universidade Federal do Ceará, UFC, Fortaleza, Ceará, Brazil.
[E]Departamento Edafoloxía y Química Agrícola, Facultade de Bioloxía, Universidade de Santiago de Compostela, Santiago de Compostela, Spain.
[F]Corresponding author. Email: toferreira@usp.br

Abstract. Wetland soils, especially those under a semi-arid climate, are among the least studied soils in the tropics. The hypersaline tidal flats on the north-eastern Brazilian coast, locally named *apicum*, are coastal wetland ecosystems in the peripheral portions of semi-arid estuaries. Despite their great ecological importance, they have been highly impacted by anthropogenic activities. Morphological and analytical data of six soil profiles, representative of the different coastal compartments (mangroves, *apicum* and coastal tablelands) of the north-eastern Brazilian coast, were examined to better understand the pedogenesis of *apicum* soils. The hypersaline tidal flat soils were classified as Typic Fluvaquents and Typic Sulfaquents with the following main characteristics: predominance of sand fraction (62–77%); presence of high-activity clays (>24 $cmol_c\,kg^{-1}$ clay); clay fraction comprising kaolinite, illite, smectite and an interstratified smectite/illite; exchangeable complex dominated by Na^+ (ESP $\geq$15%); elevated levels of salinity (electrical conductivity, EC 25–44 $dS\,m^{-1}$); alkaline pH values (7.5–9.5). The sandy texture and quartz-dominated composition of the hypersaline, tidal flat soils indicate a pedogenesis associated with the superficial addition of mineral material. This upbuilding process would have lowered the watertable (relatively to the ground level) and decreased the flooding frequency by the tides, favouring salinisation and solonisation processes at the hypersaline tidal flats. Furthermore, the still-existing hydromorphism would have promoted the maintenance of gleisation and sulfidisation. The presence of pyrite on the hyper-saline tidal flat soils further corroborates the formation of *apicum* soils from/over buried mangroves.

Additional keywords: coastal wetlands, mineralogy, soil genesis.

Received 16 October 2012, accepted 22 October 2013, published online 13 March 2014

Introduction

The terms *salt flats* (Ridd and Stieglitz 2002), *supratidal flats*, *hypersaline tidal flats* and *unvegetated flats* (Hadlich *et al*. 2009) are used to refer to coastal ecosystems on the periphery of fluviomarine plains in arid and semi-arid estuaries. These environments are common in many parts of the world (e.g. northern Australia, south-eastern Spain, western Gulf of Mexico; see Ridd and Stieglitz 2002; Álvarez-Rogel *et al*. 2007; Forbes *et al*. 2008) and in the north-eastern region of Brazil (Hadlich *et al*. 2009), where are they are called *apicum* (a native name meaning saltwater marsh originating from the Tupi-Guarani language, a Brazilian indigenous group). These environments are generally located in the supra-littoral fringes, in an intermediary position between mangroves and terrestrial environments (i.e. coastal tablelands). They generally occur in association in regions where the rainy season is concentrated in ~3 months of the year (Lebigre 2007).

These marginal environments of semi-arid tropical estuaries are marked by conditions in which water evaporation largely exceeds the precipitation rate, resulting in hypersaline environments during most of the year. According to Ridd and Stieglitz (2002), these environments cover areas that generally exceed those of mangroves in arid and semi-arid estuaries in Australia, occupying the great part of tropical semi-arid intertidal zones. Due to their physiographic position, these environments are flooded only twice a month during the spring tides, whereas mangroves are flooded twice each day (Vieillefon 1969; Zack and Román-Mas 1988; Forbes *et al*. 2008). Under these conditions, the high evapotranspiration rates, associated with low tidal flushing of accumulated salts

and negligible river discharges into estuaries, can cause high concentrations of salt in soils that may exceeding 5 times that of normal values of seawater (Hollins and Ridd 1997; Ridd and Stieglitz 2002).

According to Meireles *et al*. (2007), the formation of hypersaline tidal flats is related to the transportation of sedimentary material by waves, wind and fluvial systems, which favours the formation of sand banks in estuaries, causing the silting and the shifting of mangrove channels. The consequent decreased flooding frequency by the tides and the restricted entrance of fresh water would increase salt concentrations (Vieillefon 1969; Zack and Román-Mas 1988) and promote the formation of hypersaline tidal flats.

Most plant species do not have the physiological ability to survive in tidal flat soils due, mostly, to the elevated levels of salinity. The vegetation in these environments is normally sparse and patchy, composed of succulent halophytes (e.g. *Batis marítima* and *Portulaca oleracea*) and *Cyperaceae* and *Xyridaceae* species, and, in some areas, remnant mangrove species can be also found (Vieillefon 1969; Nascimento 1993; LABOMAR/SEMACE 2005; Meireles 2005).

Despite the poor vegetation and the apparent absence of fauna, hypersaline tidal flat environments play an important ecological role in estuaries, since they shelter several mangrove-typical species as well as other animals that seek the coastal zones during a specific phase of their life cycles (Schaeffer-Novelli *et al*. 2000). The high density of the larval population of the crab *Ucides cordatus*, generally identified in Brazilian *apicum* tidal flats environments during the beginning of summer (rainy season), is one of the examples of the ecological role of these ecosystems (Nascimento 1993). Recent studies (Schmidt 2006; Meireles *et al*. 2007) emphasise the action of these ecosystems as true 'nurseries' for some species of great ecological importance (i.e. molluscs, crustaceans and migratory birds).

Despite their ecological importance, hypersaline tidal flat environments have been greatly affected by anthropogenic activities on the north-eastern Brazilian coast. These impacts are main relate to urbanisation, deforestation and aquaculture (shrimp farming), which affect both direct and indirectly hypersaline tidal flat biological and physico-chemical properties (Meireles *et al*. 2010). Brazilian environmental protection laws prohibit shrimp farming activity in mangrove areas but are permissive, with few restrictions, of the installation of this activity in *apicum* ecosystems (BRAZIL 2012). This has caused the degradation of many hypersaline tidal flat areas by both physical occupation and the discharge of shrimp ponds effluent-rich in nutrients (Lahman and Snedaker1987; Coelho and Schaeffer-Novelli 2000).

Increasing degradation of hypersaline tidal flat environments in north-eastern Brazil has resulted in the need for basic information about their soils, essential to achieving a better understanding of the overall functioning of these ecosystems and to provide useful information for ecological and environmental studies. However, few studies have dealt directly with hypersaline tidal flat substrates using a pedological approach.

In rare edaphic studies of *apicum* environments from Brazil (Ruivo *et al*. 2005; Hadlich *et al*. 2009), its soils were classified as Arenosols and Fluvisols, due to the predominance of sand fraction and the irregular distribution of organic carbon contents with depth. In similar environments from a Mediterranean climate (region of Murcia, south-eastern Spain), Álvarez-Rogel *et al*. (2007) classified both Hypersalic Sodic Gleyic Solonchaks and Typic Aquisalids.

Thus, despite the necessity for soil information to understand fully the natural processes that take place in these environments, little is known about hypersaline tidal flats soils from Brazilian coastal areas (Schmidt 2006). The characterisation and classification of soils within these environments are essential to the conservation and sustainable management of these endangered ecosystems.

This paper contributes to the knowledge of hypersaline tidal flat (*apicum*) soils and their pedogenetic processes. The objectives of this study are to present physical, chemical, mineralogical and morphological data for representative hypersaline tidal flat soils (along with the adjacent coastal compartments—coastal tablelands and mangroves) in a semi-arid estuary of the State of Ceará, to discuss the factors and processes that govern pedogenesis in *apicum* environments and to classify the soils according to the Soil Taxonomy system (Soil Survey Staff 2010).

Materials and methods

Environmental setting

The *apicum* environment under study is on the Acaraú River estuary (Fig. 1), in the northern region of the State of Ceará (Brazil). The regional geology (at the Acaraú Basin) is characterised by crystalline rocks with a predominance of gneisses, schists, phyllites, amphibolites and slates. All of these rocks are folded and metamorphosed, with the most important batholiths located at Jaibaras Group (the main structural feature in the region), from the Precambrian (Diniz *et al*. 2008; Hesp *et al*. 2009).

The fluctuations in sea level during the Quaternary have greatly influenced the evolution of the Brazilian coastal plains (Suguio *et al*. 1985). The sea level fluctuations and paleoclimatic changes, which occurred between 22 000 and 14 000 years BP (last transgressive periods), were relevant for the formation of an extensive coastal plain, which includes: estuaries, mangroves, dune fields, lagoons, ponds and the *apicum* hypersaline tidal flat (Meireles and Raventos 2002).

The surficial geology of the estuary is characterised by fluvial and recent aeolian littoral sediments, derived from sandy-clayish and sandy sediments of the Barreiras Formation. These sediments are characterised by reddish sand, solidly compacted, with conglomerate layers in a reddish sandy matrix (Diniz *et al*. 2008). The Serra Grande Group, which borders the Acaraú Basin, consists of Phanerozoic acid rocks from the Silurian–Devonian periods and the basaltic, rhyolitic rocks of the Parapuí Formation (Almeida and Andrade Filho1999; Galvão 2002).

The climate in the region is tropical semi-arid (Fig. 1*a*; Aw according to the Köppen classification), with precipitation from January to April (Fig. 2). There are two well-defined seasons: a long and dry season in winter and a short rainy and hot season in summer (Köppen and Geiger 1928). The main vegetation unit in

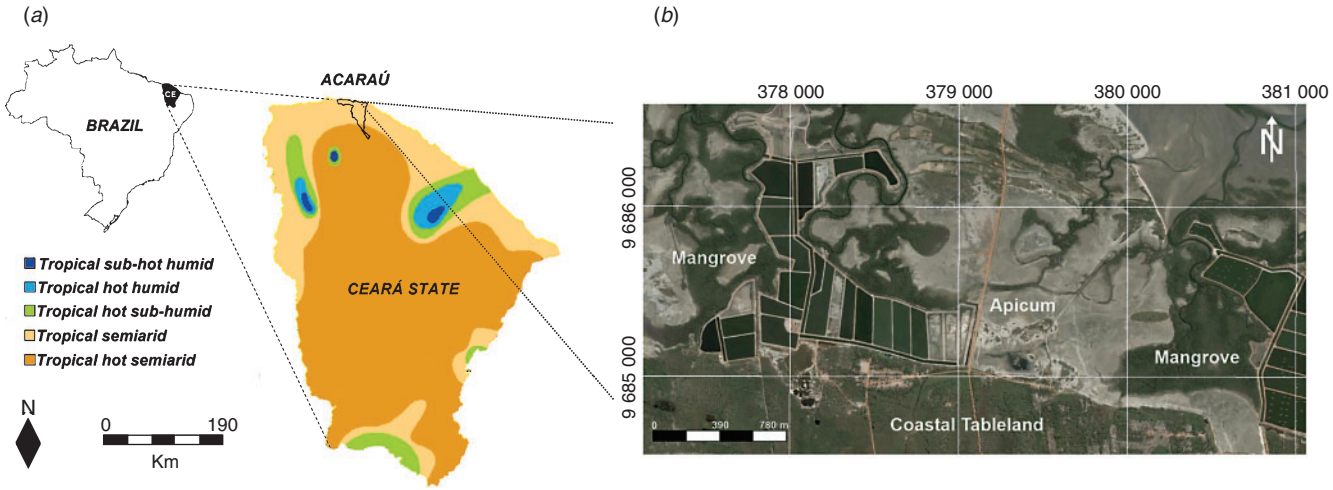

Fig. 1. (*a*) Location and climate classification map of the study site at the Ceará State, Brazil, and (*b*) an aerial photograph of the studied hyper-saline tidal flat, showing shrimp ponds within the *apicum* hypersaline tidal flat and mangrove ecosystems.

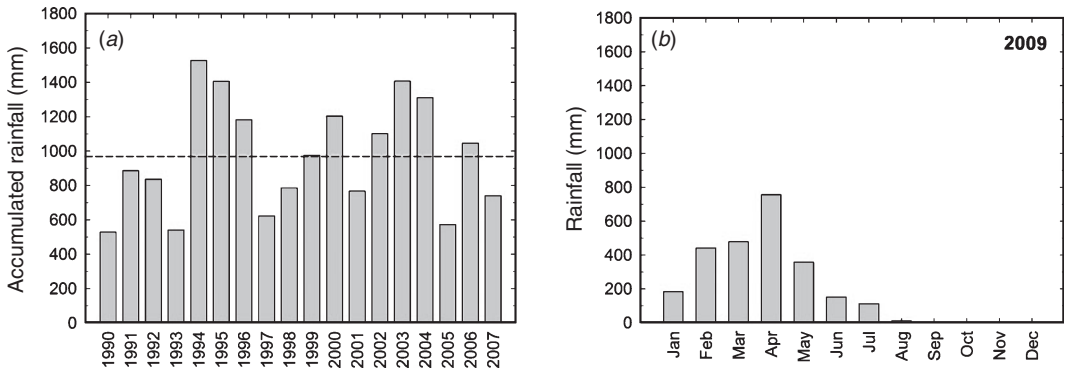

Fig. 2. (*a*) Acaraú historical precipitation records (1990–2007) and the annual average precipitation (horizontal line); (*b*) Acaraú monthly precipitation for the year of the study (2009).

the Acaraú River and its tributaries is dominated by Caatinga (a seasonal, xerophilous thorn woodland/shrubland), and the area's climate is classified as tropical hot semi-arid (Maia *et al.* 2006). The average annual precipitation is 950 mm and the average annual evapotranspiration is 1600 mm (Lobato *et al.* 2008). Harsh droughts, occasionally associated with El Niño–Southern oscillation (ENSO), are common. Furthermore, an extremely high evaporative demand may cause evaporation rates >10 mm day^{-1} (Folhes *et al.* 2009). Average annual maximum and minimum temperatures are 34 and 18°C, respectively.

The studied hypersaline tidal flat system is in the transition zone between the coastal tablelands (highlands, towards the inland areas) and the mangrove forests in the seaward position (Fig. 3). The vegetation fringing and forming patches within the Acaraú River hypersaline tidal flat is dominated by the halophyte *Batis maritima* L. (Fig. 4*f*). The *apicum* environment under study is flooded twice a month during spring tides events, which allows sea water to evaporate between periods of inundation, whereas the mangroves are flooded daily. The area is a mesotidal environment, with a diurnal tide and a maximum range of 3 m (Jimenez *et al.* 1999).

Soil sampling

Two representative soil profiles from each coastal compartment (coastal tablelands, *apicum* and mangroves; Fig. 3) were selected based on their physiographic position, constituting a toposequence. Soil profiles from coastal tablelands (P1 and P2) were at the summit position (altitudes ranging between 18 and 29 m; Fig. 3). *Apicum* soil profiles (P3 and P4) were at central part of the toposequence (footslope positions). Profile P3 occupies a higher position within the hypersaline tidal flat (2 m) in close contact with highland vegetation (coastal tableland) and is subject to less frequent tidal flushing. Soil profile P4 (altitude ~1.5 m) is closer to the mangrove forest and thus marked by more frequent tidal flooding (Fig. 3). In the adjacent mangrove forest (toeslope position), two soil profiles (P5 and P6) were nearly at sea level. The soil profile P5 was close to the mangrove creek, under a *Rhizophora* spp. forest, whereas P6 was in a more seaward position, under an *Avicennia* spp. forest (Fig. 3).

Sampling was performed during the dry season of 2009. Soil pits were dug in coastal tableland (to a depth of ~2 m) and *apicum* (to a depth of 1 m) and sampled by horizon. Mangrove soil profiles (P5 and P6) were sampled during the low tide with a

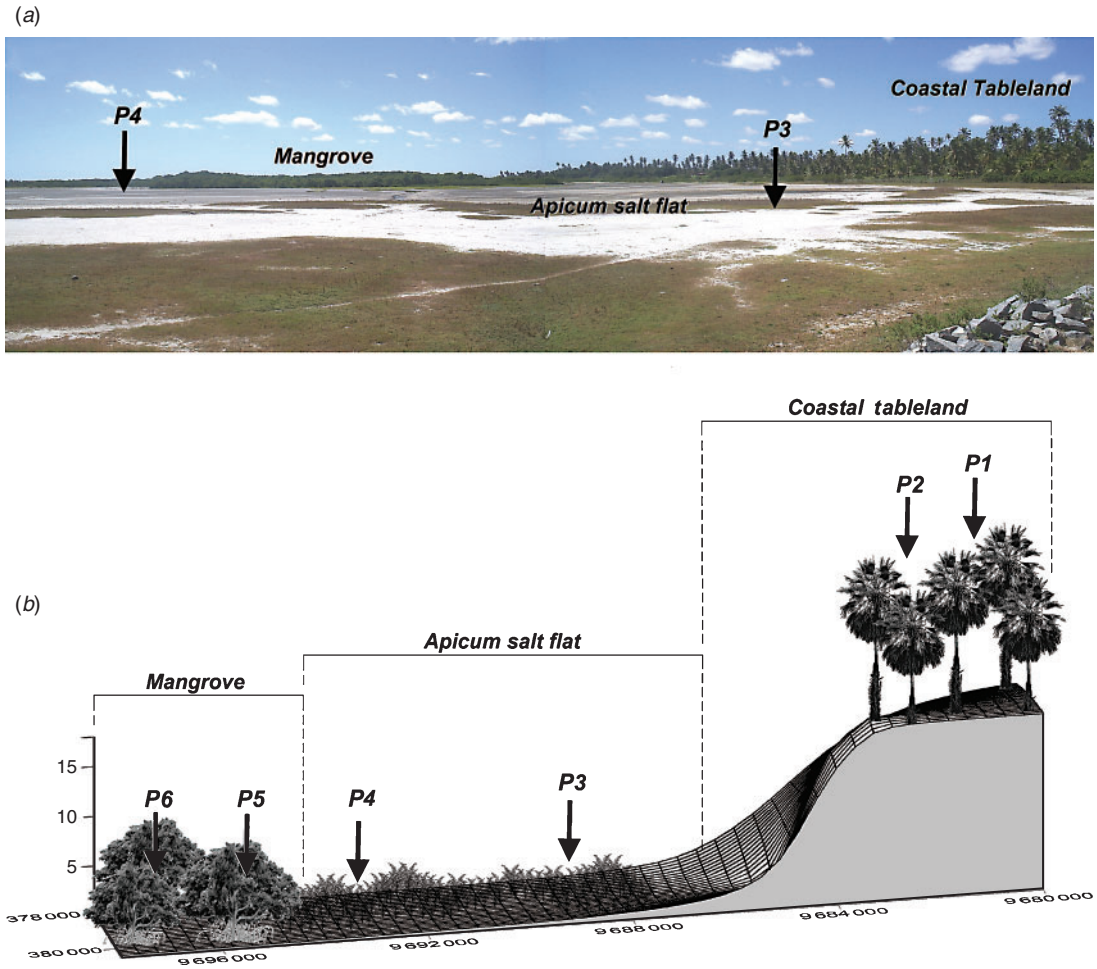

Fig. 3. (*a*) Photograph of the studied *apicum* hypersaline tidal flat showing the phytogeomorphological compartments (mangrove, *apicum* and coastal tablelands) (photo: T. O. Ferreira); and (*b*) their topographic configuration.

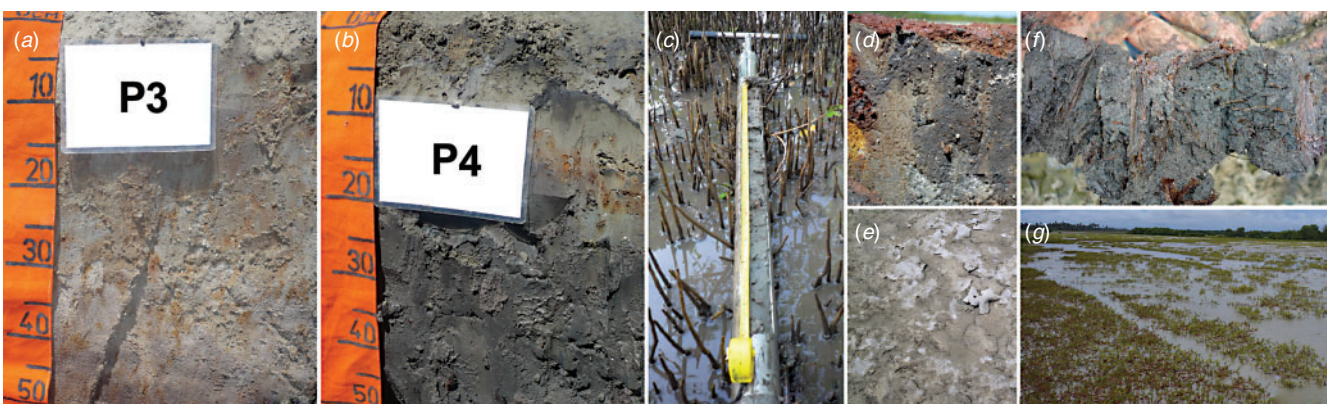

Fig. 4. Representative soil pedons of (*a*) P3 and (*b*) P4 (both hyper-saline tidal flat), and (*c*) mangrove; (*d*) a detail of the observed soil-mottling features; (*e*) mangrove plant vestiges burrowed in P4; (*f*) detail of the surface saline crust; and (*g*) *apicum* hypersaline tidal flat typical vegetation (*Batis maritime*) and the characteristic patchy soil cover. (Photos A. G. B. Marques and T. O. Ferreira.)

special sampler for flooded soils, which consisted of a 0.9-m-long stainless-steel tube of 0.1 m diameter; samples were taken at 0–0.3, 0.3–0.6 and 0.6– 0.9 m depth.

For each soil, a detailed morphological description was carried out following the guidelines proposed by Schoeneberger *et al*. (2002). Soil colours were obtained using

the Munsell Color (2000) chart. The pH and redox potential (Eh) values of all *apicum* and mangrove samples were measured in the field, after equilibrating the cores and electrodes for ~2 min. Probes were inserted in the centre of each core to avoid contact with the atmosphere. The pH values of all samples were measured using a glass electrode calibrated using pH 4.0 and 7.0 standards. The Eh was measured in the field using a platinum electrode and the final readings were corrected by adding the potential (+244 mV) of a calomel reference electrode.

Analytical procedures

In the laboratory, subsamples from *apicum* and mangrove soils were air-dried, crushed and sieved, whereas part of the samples was frozen for posterior acid sulfate soil analysis (e.g. for the determination of sulfidic material and quantification of pyritic iron). All samples from coastal tableland soils were analysed after drying, crushing and sieving procedures.

The EC was measured in saturated extracts, using dried samples (Rhoades 1996), with a conductivity meter. Total organic carbon (TOC) was determined by dry combustion of dried samples, using a LECO-CNS Model 2000 (LECO Corp., St. Joseph, MI, USA), after treatment with 6 M HCl to remove inorganic C. Also, for samples from coastal tableland soils, a combined glass–calomel electrode was used to determine pH (1 : 2.5 solid/liquid ratio) values.

Before chemical and physical analyses, the air-dried samples from *apicum* and mangrove soils were washed with 60% (v/v) aqueous ethanol to remove salts (Bower *et al*. 1952; Sumner and Miller 1996) until the silver nitrate test ($AgNO_3$ 0.05 N) indicated absence of chloride. The pipette method (Gee and Bauder 1986) was used for particle-size analysis, preceded by oxidation of organic matter with H_2O_2 (30%) by using a combination of physical (overnight shaking) and chemical (0.015 M $(NaPO_3)_6$ + 1.0 M NaOH) dispersal methods. Potential acidity (H + Al) was determined by extraction with a 1 M Ca acetate solution at pH 7 (Quaggio *et al*. 1985). Cation exchange capacity (CEC) was calculated as the sum of exchangeable cations (Ca, Mg, K, Na, and H + Al; Sumner and Miller 1996).

Exchangeable K and Na were extracted with 0.05 N HCl + 0.025 N H_2SO_4 (Mehlich I; Mehlich 1953), and exchangeable Ca, Mg and Al were extracted by shaking with 1 M KCl (1 : 5, soil : solution), from which the cations were determined by flame photometry (K and Na), atomic absorption spectrophotometry (Ca and Mg), and by titration with a standard NaOH solution (Al). The calcium carbonate equivalent was obtained by AOAC method (AOAC 1970) and Metson (1956).

In order to test for the presence of sulfidic materials, the total potential acidity (TPA) was determined after oxidation of fresh soil (mangrove and *apicum*) samples with H_2O_2 (30% at pH 5.5; 1 soil : 5 solution), followed by pH measurement, according to Konsten *et al*. (1988).

Additionally, to quantify the pyritic fraction, a partitioning of solid-phase Fe was determined using the method proposed by Lord (1982) in fresh samples. Briefly, the method consists in the extraction of two operationally defined fractions: F1, iron oxyhydroxides: extracted with 20 mL of a solution of 0.25 M sodium citrate + 0.11 M sodium bicarbonate, with 3 g of sodium dithionite then samples were shaken for 30 min at 75°C and centrifuged at 10 000 rpm (4°C) for 30 min; F2, pyrite iron: extracted with 10 mL of concentrated HNO_3, then samples were shaken for 2 h at room temperature and washed with 15 mL of ultrapure water.

Before the extraction of pyrite-Fe, samples were pre-treated with 10 M HF for 16 h under agitation to eliminate sheet silicate Fe, and concentrated H_2SO_4 was then added to eliminate Fe associated with organic matter (Lord 1982; Huerta-Díaz and Morse 1990, 1992). Between each step of the extraction procedure, samples were washed with 20 mL of ultrapure water. The degree of pyritisation (DOP) was calculated as follows:

$$\mathrm{DOP}(\%) = [(\text{pyritic Fe})/(\text{oxyhydroxides Fe} + \text{pyritic Fe})] \times 100$$

The DOP determines the percentage of reactive iron incorporated in the pyritic fraction (Berner 1970) and enables comparison between soils with different concentrations of reactive iron. The DOP was calculated by considering reactive iron (iron that can react with sulfide to form pyrite), as F1 which mainly consists of iron oxyhydroxides (Berner 1970).

Mineralogical analysis was carried out on surface and subsurface samples from the studied profiles. The mineralogical composition of the clay minerals ($\leq$2 µm) was identified by X-ray diffraction (XRD). Clay samples were prepared according to the method of Jackson (1969) and analysed as oriented aggregates after being saturated with Mg^{2+} and K^{+}. The K^{+}- saturated samples were analysed at 25°C and after heating to 350°C and 550°C for 2 h (K25°C, K350°C and K550°C, respectively), whereas the Mg^{2+}- saturated samples were processed like oriented aggregates (Mg) and were also glycerol saturate (Mg-gli). Ground sand samples were spread on a double-sided tape mounted on a glass coverslip and analysed as a random powder sample (Jackson 1969). The X-ray diffractograms were obtained with a diffractometer Shimadzu XRD 6000 (Shimadzu Corporation, Tokyo), operating at 40 kV and 20 mA using Cu-K_α radiation, a graphite crystal monochromator, at 1.5 °2 Θ min^{-1} in the 3–5 °2Θ range (for oriented aggregates) and 5–70 °2 Θ range (for random powder).

The photomicrographs of pyrite were obtained from the dense soil fraction, which was separated with bromoform ($CHBr_3$ density 2.89 g mL^{-1}). The dense sample was placed on an aluminum support for observation by scanning electron microscopy. Elemental analysis (EDS, energy-dispersive X-ray spectrum) was carried out with an Evo LS15 analyser (Carl Zeiss Microscopy GmbH, Jena, Germany). Microanalysis was carried out, after an internal calibration, using an Inca X-act Microprobe (Oxfor Instruments PL, Abingdon, UK) at 20 kV and a waiting time of 100 s.

Results and discussion

Morphological properties

Morphological, chemical and analytical data of the representative soil profiles are presented in Tables 1 and 2.

Table 1. Morphological and physical properties of the studied representative soil pedons

Mottle quantity: few (f), common (c), many (m); contrast: faint (F), distinct (D), prominent (P). Structure: massive (m), blocky structure which crumbles into single grains (sg). Boundary distinctness: clear (c); Topography: smooth (s)

Horizon	Depth (cm)	Matrix colour (Munsell)	Mottle Colour	Mottle Quantity	Mottle Contrast	Structure	Sand	Silt (%)	Clay	Texture	Boundary
P1, Typic Quartzipsamment, coastal tableland											
C	0–12	2,5YR 3/2	–	–	–	sg	95	4	1	Sand	cs
Cn1	12–50	10YR 4/2	–	–	–	sg	98	1	1	Sand	cs
Cn2	50–107	10YR 5/3	–	–	–	sg	98	1	1	Sand	cs
Cn3	107–156	10YR 5/3	–	–	–	sg	98	1	1	Sand	cs
Cn4	156–200+	10YR 5/4	–	–	–	sg	97	2	1	Sand	cs
P2, Typic Quartzipsamment, coastal tableland											
Ap	0–12	10YR 3/2	–	–	–	sg	97	2	1	Sand	cs
ACn	12–24	10YR 4/2	–	–	–	sg	96	2	2	Sand	cs
Cn1	24–46	10YR 5/3	–	–	–	sg	96	1	3	Sand	cs
C2	46–97	10YR 5/3	–	–	–	sg	96	1	3	Sand	cs
C3	97–139	10YR 6/4	–	–	–	sg	94	3	3	Sand	cs
C4	139–182	2,5YR 6/6	–	–	–	sg	93	3	4	Sand	cs
C5	182–200+	2,5YR 6/4	–	–	–	sg	93	2	5	Sand	cs
P3, Typic Fluvaquent (hyposulfidic), apicum salt flat											
Azgnk	0–6	5Y 6/2	10YR 6/4	f	P	m	81	11	8	Loamy sand	cs
2Czgnk1	6–15	5Y 6/2	10YR 5/6	c	P	m	72	13	15	Sandy loam	cs
3Czgn2	15–23	5Y 6/2	10YR 5/6	m	P	m	70	11	19	Sandy loam	cs
4Czgjn3	23–30	5Y 7/1	10YR 5/6	m	P	m	77	9	14	Sandy loam	cs
5Czgjn4	30–90+	5Y 6/1	10YR 5/6	m	P	m	89	5	6	Sand	cs
P4, Typic Sulfaquent (hypersulfidic), apicum salt flat											
Azgnk	0–10	10Y 4/1	–	–	–	m	40	29	31	Clay loam	cs
2Czgnk1	10–16	10GY 5/1	2,5YR 4/4	m	P	m	53	26	22	Sandy clay loam	cs
3Czgjnk2	16–65	5GY 4/1	–	–	–	m	62	16	21	Sandy clay loam	cs
4Czgn3	65–92+	10Y 3/1	–	–	–	m	97	2	1	Sand	cs
P5, Typic Sulfaquent (hypersulfidic), mangrove											
Cgjn1	0–30	N 4/	–	–	–	m	50	16	34	Sandy clay loam	–
Cgjn2	30–60	10Y 3/1	–	–	–	m	52	16	32	Sandy clay loam	–
Cgjn3	60–90	5GY 3/1	–	–	–	m	56	16	28	Sandy clay loam	–
P6, Typic Sulfaquent (hypersulfidic), mangrove											
Cgjnk1	0–30	10Y 3/1	–	–	–	m	35	35	30	Clay loam	–
Cgjnk2	30–60	10Y 3/1	–	–	–	m	47	33	20	Loam	–
Cgnk3	60–90	5GY 4/1	–	–	–	m	52	30	18	Loamy sand	–

Both hypersaline tidal flats soil profiles (P3 and P4) presented low chroma and gley colours throughout all horizons (Table 1, Fig. 4*a*, *b*). These colours are characteristic of gleying process, the reduction of ferric compounds under waterlogged conditions, with the production of bluish, greenish grey or whitish matrix colours (Munsell colours) (Schwertmann 1992). However, lower chroma (<2; Table 1) and the dominance of gley hues (10GY and 5GY; Table 1) in P4 indicate a more intense gleying process in this site, similar to those found in mangrove soils (Table 1, Fig. 4*c*), probably in response to the proximity to the sea, which favours longer periods of water stagnation and, thus, gleisation.

By contrast, profile P3, in an inner zone in the tidal flat (transition with coastal tablelands; Fig. 3), presented more mottling (Table 1, Fig. 4*d*), indicative of alternating periods of oxidation and reduction and thus associated with more frequent watertable fluctuations. Coastal tableland soils presented higher chroma colours (Table 1), evidencing better drainage conditions, due to their higher topographic position, sandy texture (Table 1) and, thus, higher permeability.

In the *apicum* soils, lithological discontinuities were identified from field observations of texture and soil colour and were corroborated by TOC depth profile (Table 2). Clear horizon boundaries (mostly clear and smooth, see Table 1) provided morphological evidence on the formation of these soils from material transported by fluvial and/or aeolian processes, which corroborates the hypothesis proposed by Meireles *et al*. (2007) for the formation of the *apicum* hypersaline tidal flat ecosystem. Additionally, the presence of buried mangrove plants in P4, associated to high concentrations of pyrite iron (see below), also appears to support this interpretation.

Furthermore, erosive processes in coastal tableland soils may also provide sediments to the *apicum*, establishing an interaction between both coastal compartments. The single-grained structure of coastal tableland soils (Table 1), mostly caused

Table 2. Chemical properties of the studied representative soil pedons

TOC, Total organic carbon; SB, sum of base cations; CEC, cation exchange capacity; Clay act., clay activity; V%, base saturation (V% = 100 × sum of bases/cation exchange capacity); ESP, exchangeable sodium percentage; CCE, $CaCO_3$ equivalent; EC, electrical conductivity of saturation extract; Oxy-Fe, oxyhydroxide-Fe; Pyr-Fe, pyrite-Fe; DOP, degree of iron pyritisation; n.d., not determined

Horizon	Depth (m)	TOC ($g\,kg^{-1}$)	Ca	Mg	Na	K	H+Al	SB	CEC	Clay act.	V	ESP	CCE	EC ($dS\,m^{-1}$)	Oxy-Fe	Pyr-Fe	DOP	Eh	Sulfidic material	
			($cmol_c\,kg^{-1}$)									(%)-			($\mu mol\,g^{-1}$)		(%)		Field pH	Post-ox. pH
P1, Typic Quartzipsamment, coastal tableland																				
C	0–12	13.5	0.6	0.4	0.3	0.1	2.9	1.3	4.2	–	30.8	5.9	2.6	0.3	n.d.	n.d.	n.d.	n.d.	n.d.	n.d.
Cn1	12–50	1.3	0.6	0.0	0.3	0.1	1.9	0.9	2.8	–	33.8	9.7	2.2	0.2	n.d.	n.d.	n.d.	n.d.	n.d.	n.d.
Cn2	50–107	0.6	0.6	0.4	0.3	0.0	2.1	1.4	3.5	–	39.1	9.3	2.1	0.1	n.d.	n.d.	n.d.	n.d.	n.d.	n.d.
Cn3	107–156	5.2	1.0	0.0	0.3	0.0	1.6	1.3	2.9	–	45.7	9.8	2.3	0.1	n.d.	n.d.	n.d.	n.d.	n.d.	n.d.
Cn4	156–200+	4.3	0.6	0.4	0.3	0.0	2.3	1.3	3.6	–	36.5	8.0	2.0	0.1	n.d.	n.d.	n.d.	n.d.	n.d.	n.d.
P2, Typic Quartzipsamment, coastal tableland																				
Ap	0–12	8.4	1.6	2.2	0.4	0.1	1.8	4.3	6.0	–	70.9	6.4	2.1	0.3	n.d.	n.d.	n.d.	n.d.	n.d.	n.d.
ACn	12–24	1.9	1.0	1.1	0.4	0.1	1.5	2.5	4.0	–	63.7	8.8	2.1	0.1	n.d.	n.d.	n.d.	n.d.	n.d.	n.d.
Cn1	24–46	2.7	1.0	2.4	0.3	0.1	1.1	3.8	4.9	–	78.5	6.4	3.0	0.1	n.d.	n.d.	n.d.	n.d.	n.d.	n.d.
C2	46–97	1.3	2.6	0.8	0.3	0.1	1.2	3.7	4.9	–	75.7	5.5	2.3	0.2	n.d.	n.d.	n.d.	n.d.	n.d.	n.d.
C3	97–139	3.1	0.8	2.8	0.3	0.1	1.4	4.0	5.3	–	74.5	5.4	3.4	0.1	n.d.	n.d.	n.d.	n.d.	n.d.	n.d.
C4	139–182	4.8	1.0	2.4	0.3	0.1	1.6	3.8	5.4	–	70.1	5.5	2.9	0.1	n.d.	n.d.	n.d.	n.d.	n.d.	n.d.
C5	182–200+	5.7	1.0	2.2	0.3	0.1	1.4	3.5	4.9	–	72.4	5.7	3.6	0.1	n.d.	n.d.	n.d.	n.d.	n.d.	n.d.
P3, Typic Fluvaquent (hyposulfidic), apicum salt flat																				
Azgnk	0–6	0.57	1.8	3.0	1.6	0.5	1.2	6.9	8.0	–	85.7	19.8	5.1	42.8	79.0	0.4	0.5	452	8.3	7.5
2Czgnk1	6–15	0.41	1.8	3.4	3.9	1.0	1.1	10.1	11.2	74.7	90.6	35.3	5.4	31.7	82.6	0.4	0.5	460	7.7	6.7
3Czgn2	15–23	0.41	2.0	2.8	4.1	0.9	1.5	9.8	11.3	59.5	86.7	35.8	4.7	30.9	86.1	1.4	1.6	460	8.8	6.8
4Czgjn3	23–30	0.19	1.2	2.8	2.6	0.7	1.5	7.3	8.7	62.1	82.8	29.2	3.7	28.9	110.4	16.5	13.0	403	8.9	6.4
5Czgjn4	30–90+	0.39	2.4	0.8	1.2	0.4	1.3	4.8	6.1	101.7	78.9	20.0	2.5	25.8	38.0	59.4	61.0	396	8.5	6.9
P4, Typic Sulfaquent (hypersulfidic), apicum salt flat																				
Azgnk	0–10	7.7	1.8	6.8	5.6	1.5	0.3	15.7	16.0	–	98.1	35.2	10.7	31.4	102.5	0.6	0.6	446	9.1	7.0
2Czgnk1	10–16	12.9	1.2	5.2	5.7	1.2	4.3	13.3	17.6	80.0	75.6	32.5	4.8	32.3	143.8	0.7	0.5	417	8.6	6.6
3Czgjnk2	16–65	25.8	1.6	4.4	5.8	1.1	1.8	12.9	14.7	70.0	88.1	39.6	4.6	44.0	63.3	151.1	70.5	394	5.3	1.5
4Czgn3	65–92+	0.6	0.8	2.0	4.2	0.1	4.9	7.1	12.0	–	59.4	35.3	2.2	32.9	n.d.	82.7	n.d.	n.d.	5.0	2.5
P5,Typic Sulfaquent (hypersulfidic), mangrove																				
Cgjn1	0–30	50.2	5.6	9.4	6.4	2.0	3.4	23.4	26.8	78.2	87.3	24.0	3.4	28.0	11.8	44.3	79.0	435	6.9	2.7
Cgjn2	30–60	40.0	5.8	9.8	8.5	0.2	3.9	24.2	26.4	82.0	91.7	32.0	3.3	36.3	5.7	42.2	88.1	-81	6.8	1.7
Cgjn3	60–90	33.8	9.4	7.2	8.5	0.1	4.7	25.3	28.9	103.1	87.5	29.6	2.4	37.5	n.d.	n.d.	n.d.	n.d.	n.d.	1.7
P6, Typic Sulfaquent (hypersulfidic), mangrove																				
Cgjnk1	0–30	29.8	8.2	1.4	6.4	2.0	1.6	18.0	19.6	65.3	91.9	32.7	5.6	37.2	28.8	13.0	31.1	116	7.2	2.4
Cgjnk2	30–60	23.3	9.0	11.0	7.9	1.8	1.4	29.7	31.1	155.5	95.5	25.4	6.4	50.3	6.0	40.0	87.0	64	7.1	2.0
Cgnk3	60–90	22.8	11.0	7.0	6.4	1.4	2.0	25.8	27.8	154.4	92.8	23.0	10.5	46.9	n.d.	n.d.	n.d.	n.d.	n.d.	5.5

by sandy textures (sand >90%, Table 1) and low TOC contents (Table 2), may favour this erosive process.

With regard to soil structure, both mangrove and *apicum* soils did not present recognisable macroaggregates (massive soil structures; Table 1, Fig. 4*a–c*). Despite the reduced flooding frequency by the tides and the restricted entrance of fresh water in the tidal flat (Zack and Román-Mas 1988), especially compared with mangrove forest soils, both hypersaline tidal flat soils showed weak pedality (Table 1, Fig. 4*a*, *b*). This morphological characteristic may be related to both the hydrological conditions and the plant cover. The absence of macroaggregates indicates that both P3 and P4 were subjected to an incipient physical ripening, which consists of dehydration and shrinkage, an increase of permeability, crack development, an increase in permeability and the development of soil structure (Ellis and Atherton 2003; Vermeulen *et al*. 2003), probably in response to regular flooding events. Additionally, since plant activity is a key factor for structure development and, thus, soil ripening (Ellis and Atherton 2003), the poor and patchy vegetation cover in hypersaline tidal flats (Fig. 4*g*) is probably another determinant factor for weakly structured surface horizons.

Physical properties

Soil physical properties varied widely depending on the pedon (Table 1). Sand, silt and clay contents of P3 were in the ranges 70–89, 5–13 and 6–19%, respectively, whereas in P4, contents were 40–97, 2–29 and 1–31%. A higher proportion of sand was observed in P3 (Table 1) than P4. This textural contrast between P3 and P4 may have been generated by the different physiographic positions of both profiles.

Because of its physiographic position, the sediment supply at the P3 location probably depends on both tidal action and erosion of upland (P1 and P2) soils by pluvial discharge. Thus, the coarser texture of P3 is probably related to its location close to the transition between hypersaline tidal flats and coastal tablelands (Fig. 3*b*), where soils are more subject to input of eroded material from surrounding upland soils (Marques 2010). The presence of soils derived from the sandy-clay sediments of the Barreiras Group in the coastal tablelands, such as P1 and P2 (Typic Quartzipsamments, Table 1) and sandy clay loam Ultisols (Lima *et al*. 2006; Vieira *et al*. 2012), is in accordance with the ideas expressed above. This sediment input from upland soils may also explain the sandy-clay–loam texture in the mangrove soil profile P5, which is in closer contact with the *apicum*. By contrast, higher clay contents in P6 (Table 1) may evidence the dominance of an estuarine depositional environment (less energetic).

Another factor contributing to the sand dominance in profiles P3 and P4 is the theory of aeolian influence on *apicum* hypersaline tidal flat formation (Meireles *et al*. 2007). In fact, aeolian sediment transport and dune migration in Ceará coastal zones are known as key factors in the geomorphological dynamics of intertidal areas, especially because dunes play an important role in the coastal sedimentary budget (Jimenez *et al*. 1999).

The dominant winds and the rainfall regime of the Ceará coast are mostly ruled by the intertropical convergence zone (ITCZ). Thus, when the ITCZ is in its northernmost position (usually between August and December), intense south-easterly winds (average velocities of 7.75 m s^{-1}) and low rainfall dominate the coastal zone (Sauermann *et al*. 2003). Previous studies have reported average dune migration rates of 17.5 m $year^{-1}$ and bulk sediment transport rates of 90–100 m^3 m^{-1} $year^{-1}$ (Jimenez *et al*. 1999). Therefore, the great wind intensity along the Ceará coast would promote changes in the morphodynamics of the estuarine system, causing high rates of dune migration, siltation of tidal channels and the supply of sediments to sand banks, which would evolve to *apicum* hypersaline tidal flats (IBAMA 2005; FUNCEME 2009).

Chemical properties

In *apicum* and mangrove soils, the ratio of CEC to clay content, a commonly used proxy for clay activity, indicates the presence of high activity clays in representative profiles from both compartments, as judged by the values of >24 $cmol_c$ kg^{-1} clay (Table 2). In fact, the XRD data of the soils from P3, P4, P5 and P6 showed the presence of 2 : 1 minerals (smectite, illite, vermiculite and interstratified smectite/illite; Fig. 5). Both hypersaline tidal flat soil profiles presented an exchange complex dominated by sodium ($Na^+ > Mg^{2+} > Ca^{2+} > K^+$; Table 2), a condition also observed in mangrove soils. Considerably lower CEC and base saturation values in coastal tableland soils are related to their coarser textures and better drainage conditions.

The highest values of Na^+ (ESP $\geq$15%; Soil Survey Staff 2010), recorded in *apicum* soils, are related to the flooding events by sea water, the high evaporative environment and low relief (2 m above sea-level), which promotes the stagnation of water and thus accumulation of bases by preventing leaching.

The EC values in *apicum* soils ranged from 25 to 44 dS m^{-1}, with the highest values corresponding to the soil profile P4 (Table 2). The EC values showed a clear increase towards seaward positions where the hypersaline tidal flat soils come in closer contact with seawater, and the mangrove ecosystem. However, the EC values found in *apicum* and mangrove soil profiles are considerably higher than recorded in soils from other coastal ecosystem environments. In fact, the EC values in the present study were 140% higher than in mangrove soils from other parts of Brazil (Ferreira *et al*. 2010; Prada-Gamero *et al*. 2004).

These data are evidence of an intense salinisation process in hypersaline tidal flat soils, probably due to an association of both its higher physiographic position in relation to other coastal environments (i.e. mangroves and salt marshes) and the high evapotranspiration rates. The more elevated position of hypersaline tidal flat would promote a low flooding frequency (mostly related to spring tides events), while the high evapotranspiration rates (Lobato *et al*. 2008) would cause the evaporation of saline water (Zack and Román-Mas 1988; Ridd and Stieglitz 2002) and the high salt concentration (Zack and Román-Mas 1988). In fact, both hypersaline tidal flat soils presented white and wavy surface salt crusts (Fig. 4*e*) characteristic of an intense salinisation process (Hamdi-Aissa *et al*. 2004; Joeckel and Ang Clement 2005; Zenova *et al*. 2007).

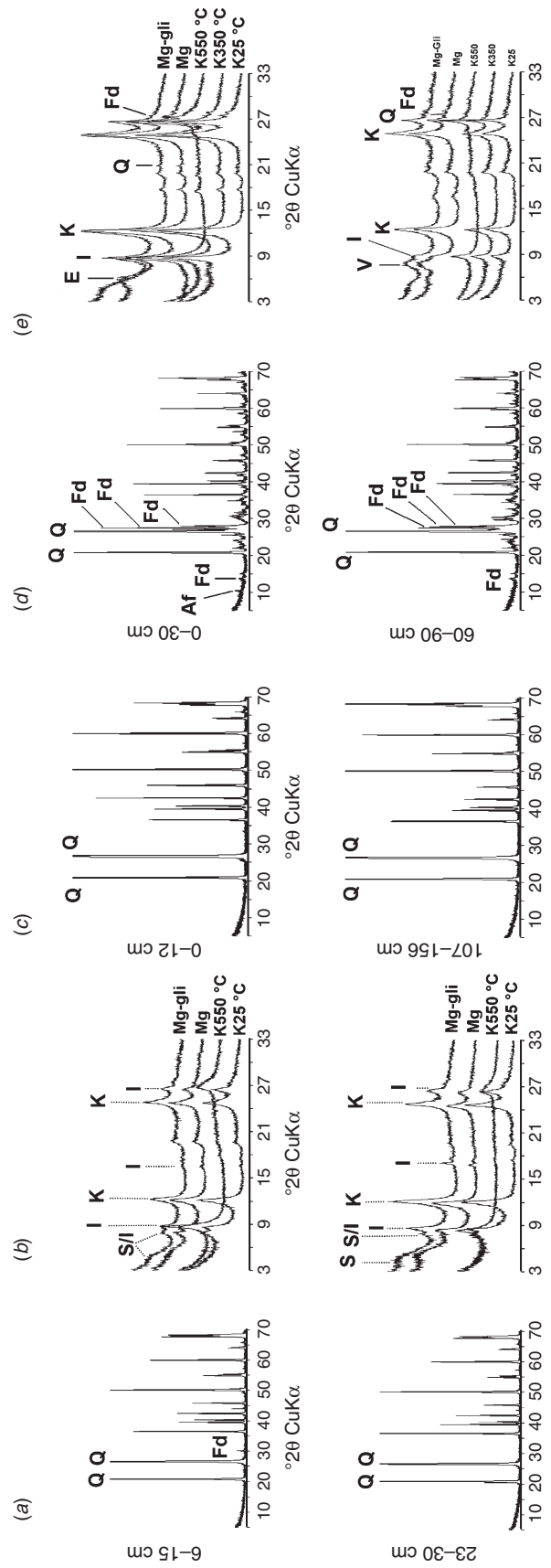

Fig. 5. X-ray diffraction (XRD) patterns of surficial (6–15 cm) and subsurficial (23–30 cm) (*a*) sand and (*b*) clay samples from hyper-saline tidal flats soils; (*c*) XRD patterns of surficial (0–12 cm) and subsurficial sand samples from coastal tableland soils (107–156 cm); XRD patterns of surficial (0–30 cm) and subsurficial (60–90 cm) (*d*) sand and (*e*) clay samples from mangrove soils. Q, Quartz (0.426; 0.334 nm); Fd, feldspar (0.296 nm); S, smectite (1.932 nm); S/I. interstratified smectite/illite (1.997; 1.132 nm); I, illite (0.337; 0.500; 1.021 nm); K, kaolinite (0.357; 0.722 nm).

Furthermore, the highest exchangeable sodium percentage (ESP) (>20%) in *apicum* soils indicates an intense solonisation/sodication process, which is probably favoured by the lower solubility of calcite compared with other salts that are commonly are found in coastal and arid environments, i.e. gypsum ($CaSO_4.2H_2O$), anhydrite ($CaSO_4$), halite (NaCl), sylvite (KCl), etc. In this case, the precipitation of calcium as $CaCO_3$ would remove dissolved and exchangeable Ca^{2+} and promote its replacement by Na^+ (reaction 1; Langmuir 1997; van Breeman and Buurman 2002):

$$Ca^{2+}{}_{(ex)} + 2Na^{+}{}_{(aq)} + 2HCO_3{}^{-} \rightarrow CaCO_3 + H_2O + 2Na^{+}{}_{(ex)} \quad (1)$$

In fact, the near-neutral and alkaline conditions (pH 7.7–9.1) (see McBride 1994; Chesworth 2008) found in most horizons from both *apicum* soils (except the deeper horizons in P4) are evidence that the system is buffered by the dissolution and precipitation of $CaCO_3$ (reaction 2), which is consistent with the high calcium carbonate content found in these horizons (Table 2).

Under these conditions, practically all calcium is precipitated as calcite and the soil solution remains dominated by $HCO_3{}^{-}$ and Na^+, as the counter ion. As the calcite precipitation takes place, in response to the high evapotranspiration rates (especially in *apicum*, due to its higher topographic position when compared with mangrove), the concentration of $CO_3{}^{2-}$ strongly increases, leading to high pH values (pH >8.5) (for more detail see van Breeman and Buurman 2002; Chesworth 2008), and to an alkalisation process:

$$CaCO_3 + H^+ \leftrightarrow Ca^{2+} + HCO_3{}^{-} \quad (2)$$

A completely different situation was found in subsurface horizons (below 16 cm) from P4, where field pH values dropped to <5.5 (Table 2) and oxidation pH to <3. As previously mentioned, these deeper *apicum* soil horizons are probably related to a buried mangrove soil. The low oxidation pH values and the presence of pyrite in both studied mangrove soils (Table 2) support this hypothesis. In fact, previous work in this area (Marques 2010; Araújo Jr *et al*. 2012; Nóbrega *et al*. 2013), as well as in other parts of Brazil (Ferreira *et al*. 2007), recorded high concentrations of iron sulfides, especially pyrite (FeS_2) and meta-stable sulfides, i.e. AVS (FeS, Fe_3S_4) in mangrove soils. The oxidation of these iron sulfides may have caused the lower field and oxidation pH in these subsurface horizons from *apicum* soils (Table 2). Thus, the watertable oscillation, evidenced by the presence of mottles (Table 1), indicates alternating redox conditions, which may be responsible for sulfide oxidation upon aeration during low watertable events (reactions 3, 4, 5 and 6) (Stumm and Morgan 1996).

$$FeS_2(s) + 7/2\ O_2 + H_2O \leftrightarrow Fe^{2+} + 2SO_4{}^{2-} + 2H^+ \quad (3)$$

$$Fe^{2+} + 1/4\ O_2 + H^+ \leftrightarrow Fe^{3+} + 1/2H_2O \quad (4)$$

$$Fe^{3+} + 3H_2O \leftrightarrow Fe(OH)_3(s) + 3H^+ \quad (5)$$

$$FeS_2(s) + 14Fe^{3+} + 8H_2O \leftrightarrow 15Fe^{2+} + 2SO_4{}^{2-} + 16H^+ \quad (6)$$

For *apicum* soils, the oxidation pH values (Table 2) decreased to <4.0 only in P4 (Table 2), indicating the presence of sulfidic material, as established by Soil Survey Staff (2010). However, a pronounced drop in the pH was recorded in most *apicum* soil samples upon exposure to oxidising conditions (Table 2), which is clearly related to the presence of pyrite-Fe obtained from the sequential extraction method (Table 2; P3, 59 µmol g^{-1}; and P4, 151 µmol g^{-1}).

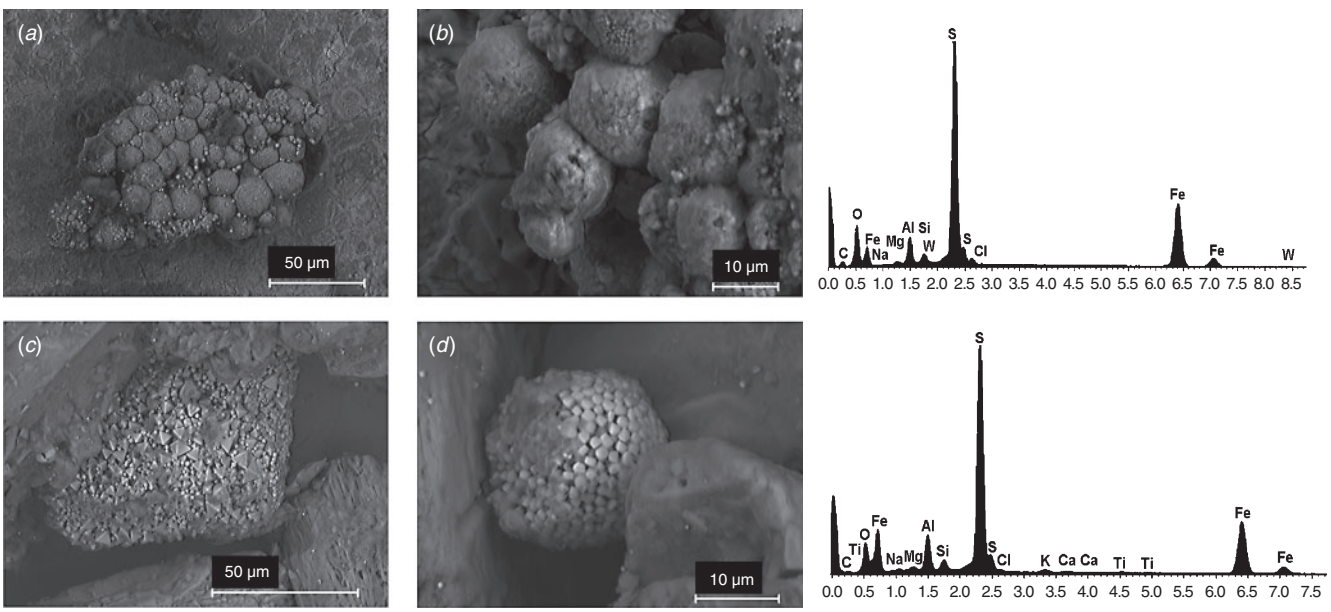

Fig. 6. Scanning electron micrographs showing different pyrite morphologies from the deeper layers of (*a*, *b*) hypersaline tidal flat soils and (*c*, *d*) mangrove soils, along with EDS spectrum showing intense iron and sulfur peaks.

The presence of pyrite-Fe at the hypersaline tidal flats soils was evident mainly in the deepest layers of P3 and P4 (Table 2), probably related to the presence of an old buried mangrove, which is consistent with the formation of *apicum* hypersaline tidal flat from siltation of tidal channels (Meireles *et al*. 2007) and mangrove fringes. The presence of what appear to be degraded pyrite framboids in the deeper horizons of both *apicum* soils (Fig. 6) is consistent with this idea.

Previous studies on soils from another typical transitional ecosystem between mangroves and the highlands (locally called *restinga* forests) have recorded degraded pyrite framboids, which were attributed to a buried mangrove facies (Gomes *et al*. 2007*a*, 2007*b*). Additionally, in the subsurface layers the more reducing conditions may have favoured the preservation of the *sulfidic material* or even active sulfidisation. The high degree of iron pyritisation (DOP) obtained in these *apicum* deeper horizons (Table 2; 61 and 70.5% for P3 and P4, respectively), also support the latter hypothesis.

The morphological differences between pyrites from *apicum* and mangrove soils (Fig. 6) seem to be a result of more oxidising conditions in the former (Eh >400 mV, Table 2). In *apicum* soils, the crystallite edges of most pyrites are not sharp (Fig. 6*a*, *b*). By contrast, in mangrove soils, pyrites present well-defined crystal edges (Fig. 6*d*, *e*), probably due to less oxidising conditions in deeper layers (Eh <100 mV). These morphological differences may also be related to the formation of iron oxyhydroxide coatings on the surface of pyrite framboids from *apicum* soils, also in response to oxidation (see Belzile *et al*. 1997; Huminicki and Rimstidt 2009; Torrentó *et al*. 2010). These coatings may also have prevented total pyrite oxidation, which would be expected under the oxic conditions found in *apicum* soils (Table 2).

On the other hand, the pyrite in surface layers of hypersaline tidal flats soils would have been almost completely oxidised (DOP <1%, Table 2) in response to the lower watertable levels established after the sedimentation events followed by a surface elevation (upbuilding). Because of this oxidation process, the produced dissolved Fe would precipitate as iron oxyhydroxides (see Ferreira *et al*. 2007). The highest concentrations of Fe-oxyhydroxides in both *apicum* profiles (Table 2; P3, 38–110 $\mu mol\ g^{-1}$; P4, 63–143 $\mu mol\ g^{-1}$) and low DOP (Table 2; P3, 0.5–1.6%; P4, 0.5–0.6%) compared with those found in mangrove soils corroborate this hypothesis. In fact, the processes of vertical accretion and surface elevation have been pointed out as important factors for mangrove dieback in other estuarine areas of the world (Rogers *et al*. 2005).

Mean TOC contents varied from 3.9 to 11.8 $g\ kg^{-1}$ in P3 and P4, respectively. In both hypersaline tidal flat soil profiles, the TOC contents presented an irregular depth distribution pattern (Table 2), which corroborates the previously mentioned burial hypothesis. The relatively high TOC contents found in deeper layer in both *apicum* profiles (Table 2) are probably related to the existence of mangrove plant vestiges in subsurface horizons (i.e. P4, 3Czgjnk2; Fig. 4*f*). In fact, Meireles and Raventos (2002) identified ancient mangrove deposits (with ages of ~310 ± 45 years BP) covered by recent marine terraces on the eastern coast of Ceará (Brazil). This record of buried mangroves is consistent with the characteristics observed in P4, where buried plant material was found at 10–65 cm depth. Previous studies from other parts of Brazil (Nascimento 1993; Ucha *et al*. 2008; Hadlich *et al*. 2010) and the world (Marius 1985; Marchand *et al*. 2011) have also documented the existence of buried mangrove tissues in similar tidal flats (for further details, see Marques *et al*. 2013). It is noteworthy that these higher TOC contents in deeper layers would have favoured pyrite formation, since organic matter is a key factor for maintaining the activity of sulfate-reducing bacteria (Ferreira *et al*. 2007). This affirmation is consistent with the data of the sequential extraction (pyrite-Fe; Table 2).

The morphological, chemical and physical characteristics of the studied profiles were used to classify the soils taxonomically (Tables 1 and 2). According to the Soil Taxonomy (Soil Survey Staff 2010), the soils are classified as Entisols. The coastal tableland soils (P1 and P2) were classified as Typic Quartzipsamments due to their sandy composition (Table 1), mainly comprising quartz (Fig. 5*c*).

With regard to *apicum* and mangrove soils, profiles showed low chroma colours (gleyed horizons) and redoximorphic features (Fig. 4*a*, *b*, *d*) in response to the saturation and reduction, thus, indicating an aquic condition. The *sulfidic material* was applicable only for P4, P5 and P6, due to the insufficient pH decrease in P3 (after exposure to oxidising conditions) and due to the relatively high amounts of calcium carbonate equivalent (Soil Survey Staff 2010). However, it must be restated that considerable amounts of pyrite were found in the subsurface layers of all four soils (Table 2), along with pyrite framboids (Fig. 6*a*, *b*). According to Sullivan *et al*. (2010), P3 can be classified as a hyposulfidic soil since it did not present a strong acidification after the oxidative process (Table 2). The Sullivan *et al*. (2010) classification scheme seems adequate for hypersaline tidal flats soils with high $CaCO_3$ contents. By contrast, according to the same classification scheme, P4, P5 and P6 would be classified as hypersulfidic soils, indicating their strong acidification potential.

However, in Soil Taxonomy (Soil Survey Staff 2010), P3 would be classified as a Typic Fluvaquent due to the irregular decrease in content of organic carbon with depth (Table 2). Despite the fact that P4 presented the same organic carbon irregularly with increasing depth, this soil (and both mangrove soils, P5 and P6) would be classified as a Typic Sulfaquent due to the presence of *sulfidic material* evidenced by a sharp decrease in pH values (≤4.0; Soil Survey Staff 2010). Although most soils were adequately classified, the authors propose the inclusion of the subgroup '*Fluventic*' in the Sulfaquent great group.

Mineralogical data

The XRD patterns for hypersaline tidal flats and mangrove soil profiles showed the same sand and clay mineralogy (Fig. 5*a*, *b*, *d*, *e*). In the sand samples from both hypersaline tidal flats and mangrove soil profiles, quartz appeared as the dominant mineral (d-spacing 0.334, 0.426 nm) followed by traces of feldspar (P3: 0.292 nm; P4: 0.296 nm; P5: 0.324 nm; P6: 0.321, 0.325, 0.330, 0.334, 0.653 nm). The dominance of quartz in both soils is probably related both to sand derived from dune migration and to the downhill erosion of the sandy-clay sediments (Lima *et al*. 2005; Sucupira *et al*. 2006) of the Barreiras Group (at upstream

coastal tableland). In fact, the mineralogical composition of the coastal tableland soils is composed, essentially, of quartz (Fig. 5*c*), indicating that these soils are a potential source of sediments to the coastal plain.

The clay mineral composition of hypersaline tidal flat soils primarily consisted of kaolinite (0.357, 0.722 nm; which collapsed after heating at 550°C), interstratified smectite/illite (S/I; 1.132, 1.997 nm), illite (1.00, 0.500, 0.334 nm) and smectite (1.48 and 1.932 nm, after glycerol solvation), the last especially at depth. This mineral assemblage is consistent with the assemblage of the mangrove soils (P5 and P6; Fig. 5*e*), and with the assemblage of other mangrove soils (Souza-Júnior *et al*. 2008; Ferreira *et al*. 2010) from different sites on the Brazilian coast. This fact further corroborates the contribution of buried mangrove soils to the pedogenesis of *apicum* hypersaline tidal flat soils.

In the studied hypersaline tidal flat soils the kaolinite is probably related to an allochthonous origin, since soils from the coastal tablelands mainly comprise kaolinite and quartz (Corrêa *et al*. 2008; Giarola *et al*. 2009). On the other hand, smectites in these estuarine environments can be either detrital or authigenic. The authigenic origin may be related to the transformation of illite, due to the oscillating redox conditions (Velde and Church 1999), or the transformation of kaolinite into smectite in response to the marine influence and poor drainage (Vilhena *et al*. 2010). Additionally, the poor drainage associated with high concentrations of silica and basic cations (Ca^{2+} and Mg^{2+}) may favour the bisiallitisation process and, thus, smectite formation (Chamley 1989). The detrital origin may be related to the terrestrial soils around the studied estuarine environment, which are under a semi-arid climate and may contain 2 : 1 minerals (both smectite and illite). The mixed-layer smectite/illite in superficial layers may be related to a transformation process, which according to Velde and Church (1999) takes place in response to the under-saturation and hypersalinisation associated with the increased concentration of cations from sea water in the upper 10 cm, and also to the oscillating redox conditions (Velde and Church 1999).

Conclusions

The results show that hypersaline tidal flats soils are characterised by a sandy texture and quartz-dominated composition as a result of the coastal morphodynamic associated with the deposition of sandy material by wind action (e.g. dune deflation or migration) and burial of a former mangrove. However, despite the simple mineralogical composition, these ecosystems present a great diversity of processes, reflected by the contrasting acid–base conditions. The strong pH oscillation between soils and depths reflects the heterogeneity and complexity of the pedogenetic processes. The results show that in surface horizons, the most significant processes are the accumulation of sodium salts (solonisation) and the precipitation of calcium carbonates, which buffers the system pH. In addition, acidic pH values found in deeper layers correspond to the oxidation of *sulfidic material* probably associated with buried mangrove soils.

This burial process would have triggered an upbuilding (allochthonous superficial addition of mineral materials to the top of the soil), lowering the watertable and decreasing the flooding frequency by tides. The mineralogical data, characterised by detrital kaolinite and autochthonous pyrite, corroborate the post-burial pedogenesis theory. These new conditions associated with the high evapotranspiration rates would have intensified the accumulation of salts and, thus, salinisation and solonisation processes. Additionally, the still existent hydromorphism (especially in deeper layers), mainly related to periodic tidal flooding and the higher physiographic position in relation to the surrounding mangrove, would favour gleisation, the preservation of pyrite and, probably, the maintenance of sulfidisation process at minimum rates.

The pedogenetic evidence presented here is fundamental to a better understanding of the general functioning of hypersaline tidal flat ecosystems and may also provide useful information for the environmental studies focussed on conservation and sustainable management of these ecosystems in Brazil. Thus, the diversity of pedogenetic processes presented in this paper seems to be an important contribution to the knowledge *apicum* soils, an ecosystem that is still poorly studied (especially from a pedological point of view) and heavily threatened, despite the its great importance for conservation of coastal natural resources in north-eastern Brazil. Future pedological studies should aim to provide further information on the connections between hypersaline tidal flats and mangrove ecosystems in order to improve environmental policies and conservation laws, which should aim for the protection of these equally important ecosystems.

Acknowledgements

The first author benefited from a scholarship from Coordenação de Aperfeiçoamento de Pessoal de Nível Superior, CAPES. The present study was financed by the Brazilian Government (CNPq).

References

Almeida RA, Andrade Filho JF (1999) A suíte magmática Parapuí—Sobral-CE: Petrologia e posição estratigráfica. *Revista de Geologia UFC* **12**, 5–28.

Álvarez-Rogel J, Carrasco L, Marín CM, Martínez-Sanchez JJ (2007) Soils of a dune coastal salt marsh system in relation to groundwater level, micro-topography and vegetation under a semiarid Mediterranean climate in SE Spain. *Catena* **69**, 111–121. doi:10.1016/j.catena.2006.04.024

AOAC (1970) 'Official methods of the Association of Agricultural Chemists.' 11 edn (Association of Official Agricultural Chemists: Washington, DC)

Araújo Jr JMC, Otero XL, Marques AGB, Nóbrega GN, Silva JRF, Ferreira TO (2012) Selective geochemistry of iron in mangrove soils in a semiarid tropical climate effects of the burrowing activity of crabs *Ucides cordatus* and *Uca maracoani*. *Geo-Marine Letters* **32**, 289–300. doi:10.1007/s00367-011-0268-5

Belzile N, Maki S, Chen YW, Goldsack D (1997) Inhibition of pyrite oxidation by surface treatment. *The Science of the Total Environment* **196**, 177–186. doi:10.1016/S0048-9697(96)05410-1

Berner RA (1970) Sedimentary pyrite formation. *American Journal of Science* **268**, 1–23. doi:10.2475/ajs.268.1.1

Bower CA, Reitemeier RF, Fireman M (1952) Exchangeable cation analysis of saline and alkali soils. *Soil Science* **73**, 251–262. doi:10.1097/00010694-195204000-00001

BRAZIL (2012) Federal law N°12.727, October 17th Brasília, DF: Diário Oficial da República Federativa do Brasil, 28 maio 2012. Available at: http://www.planalto.gov.br/ccivil_03/_ato2011-2014/2012/Lei/L12727.htm

Chamley H (1989) 'Clay sedimentology.' (Springer-Verlag: Berlin)

Chesworth W (2008) 'Encyclopedia of soil science.' (Springer: Dordrecht, the Netherlands)

Coelho C, Jr, Schaeffer-Novelli Y (2000) Considerações teóricas e práticas sobre o impacto da carcinocultura nos ecossistemas costeiros brasileiros. In: 'Mangrove 2000: Sustainable use of estuaries and mangrove: challenge and prospect' (CD-Rom). (International Society for Mangroves Ecosystem (ISME): Recife, Brazil)

Corrêa MM, Ker JC, Barrón V, Torrent J, Fontes MPF, Curi N (2008) Crystallographic properties of kaolinite soils from coastal tablelands: the Amazon and the great bay "Reconcavo Baiano". *Revista Brasileira de Ciencia do Solo* **5**, 1857–1872.

Diniz SF, Moreira CA, Corradini FA (2008) Erosive susceptible in low course of Acaraú river-CE. *Geociências* **3**, 355–367.

Ellis S, Atherton JK (2003) Properties and development of soils on reclaimed alluvial sediments of the Humber Estuary, Eastern England. *Catena* **52**, 129–147. doi:10.1016/S0341-8162(02)00179-0

Ferreira TO, Otero XL, Vidal-Torrado P, Macías F (2007) Redox processes in mangrove soils under rhizophora mangle in relation to different environmental conditions. *Soil Science Society of America Journal* **71**, 484–491. doi:10.2136/sssaj2006.0078

Ferreira TO, Otero XL, Souza Junior VS, Vidal-Torrado P, Macías F, Firme LP (2010) Spatial patterns of soil attributes and components in a mangrove system in Southeast Brazil (São Paulo). *Journal of Soils and Sediments* **10**, 995–1006. doi:10.1007/s11368-010-0224-4

Folhes MT, Rennó CD, Soares JV (2009) Remote sensing for irrigation water management in the semi arid Northeast of Brazil. *Agricultural Water Management* **96**, 1398–1408. doi:10.1016/j.agwat.2009.04.021

Forbes JM, Zhang X, Palo S, Russell J, Mlynczak M, Mertens CJ (2008) Tidal variability in the ionospheric dynamo region. *Journal of Geophysical Research* **113**, A02310. doi:10.1029/2007JA012737

FUNCEME (2009) 'A zona costeira do estado do Ceará: compartimentação geoambiental e antropismo.' (Fundação Cearense de Meteorologia e Recursos Hídricos: Fortaleza, CE, Brazil)

Galvão CC (2002) Mapeamento geológico estrutural da região nordeste de Santana do Acaraú-CE, ênfase a deformação frágil. MSc Thesis, Universidade Federal do Rio Grande do Norte: Natal, RN, Brazil.

Gee GW, Bauder JW (1986) Particle-size analysis. In 'Methods of soil analysis. Part 1. Physical and mineralogical methods'. 2nd edn. pp. 383–411. (American Society of Agronomy, Soil Science Society of America: Madison, WI, USA)

Giarola NFB, Lima HV, Romero RE, Brinatti AM, Silva AP (2009) Crystallography and Mineralogy of the Clay Fraction of Hardsetting Horizons in Soils of Coastal Tablelands in Brazil. *Revista Brasileira de Ciencia do Solo* **33**, 33–40. doi:10.1590/S0100-06832009000100004

Gomes HF, Vidal-Torrado P, Macías F, Gherardi B, Otero XL (2007*a*) Soils under restinga vegetation on the Cardoso Island (SP). I - characterization and classification. *Revista Brasileira de Ciencia do Solo* **31**, 1563–1580. doi:10.1590/S0100-06832007000600033

Gomes HF, Vidal-Torrado P, Macías F, Souza Júnior VS, Otero XL (2007*b*) Soils under restinga vegetation on the Cardoso Island (SP). II – mineralogy of silt and clay fractions. *Revista Brasileira de Ciencia do Solo* **31**, 1581–1589. doi:10.1590/S0100-06832007000600034

Hadlich GM, Ucha JM, de Oliveira TL (2009) Distribuição de apicuns e de manguezais na Baía de Todos os Santos, Bahia, Brasil. Anais do XIV Simpósio Brasileiro de Sensoriamento Remoto v. 1. p. 4607–4614.

Hadlich GM, Celino JJ, Ucha JM (2010) Physical–chemical differentiation between supratidal salt flats, mangroves and hillsides in the Todos os Santos Bay, Northeast Brazil. *Geociências* **29**, 633–641.

Hamdi-Aissa B, Valles V, Aventurier A, Ribolzi O (2004) Soils and brine geochemistry and mineralogy of hyperarid desert playa, Ouargla Basin, Algerian Sahara. *Arid Land Research and Management* **18**, 103–126. doi:10.1080/1532480490279656

Hesp PA, Maia LP, Claudino-Sales V (2009) The Holocene Barriers of Maranhão, Piauí and Ceará States, Northeastern Brazil. In 'Geology and Geomorphology of Holocene Coastal Barriers of Brazil'. pp. 325–343. (Springer-Verlag: Berlin, Heidelberg)

Hollins S, Ridd PV (1997) Evaporation over a tropical tidal salt flat. *Mangroves and Salt Marshes* **1**, 95–102. doi:10.1023/A:1009971800974

Huerta-Díaz MA, Morse JW (1990) A quantitative method for determination of trace metals in anoxic marine sediments. *Geochimica et Cosmochimica Acta* **29**, 119–144.

Huerta-Díaz MA, Morse JW (1992) Pyritization of trace metals in anoxic marine sediments. *Geochimica et Cosmochimica Acta* **56**, 2681–2702. doi:10.1016/0016-7037(92)90353-K

Huminicki DMC, Rimstidt JD (2009) Iron oxyhydroxide coating of pyrite for acid mine drainage control. *Applied Geochemistry* **24**, 1626–1634. doi:10.1016/j.apgeochem.2009.04.032

IBAMA (2005) 'Diagnóstico da carcinicultura no estado do Ceará.' (Instituto Brasileiro de Meio Ambiente e dos Recursos Naturais Renováveis: Brasilia, Distrito Federal)

Jackson ML (1969) 'Soil chemical analysis (advanced course).' (Prentice Hall: Englewood Cliffs, NJ)

Jimenez JA, Maia LP, Serra J, Moeia J (1999) Aeolian dune migration along the Ceará coast, north-eastern Brazil. *Sedimentology* **46**, 689–701. doi:10.1046/j.1365-3091.1999.00240.x

Joeckel RM, Ang Clement BJ (2005) Soils, surficial geology, and geomicrobiology of saline-sodic wetlands, North Platte River Valley, Nebraska, USA. *Catena* **61**, 63–101. doi:10.1016/j.catena.2004.12.006

Konsten CJM, Adriesse W, Brinkman R (1988) A field laboratory method to determine total potential and actual acidity in acid sulphate soils. In 'Selected Papers of the Dakar Symposium on Acid Sulphate Soils'. Vol. 44, pp. 106–134..(International Institute for Land Reclamation and Improvement: Wageningen, the Netherlands)

Köppen W, Geiger R (1928) 'Klimate der erde.' (Wall-map 150 cm × 200 cm) (Verlag Justus Perthes: Gotha, Germany).

LABOMAR/SEMACE (2005) Mapeamento as unidades geoambientais da zona costeira do Estado do Ceará. Instituto de Ciências do Mar/ Superintendência Estadual do Meio Ambiente Programa: Zoneamento Ecológico e Econômico da zona costeira do Ceará, Brasil. Fortaleza, CE, Brazil.

Lahman EJ, Snedaker SC (1987) Structural comparisons of mangrove forest near shrimp ponds in Southern Ecuador. *Interciencia* **5**, 240–243.

Langmuir D (1997) 'Aqueous environmental geochemistry.' (Simon & Schuster: New York)

Lebigre JM (2007) Les marais à mangrove et lês tannes. Available at: http://www.futura-sciences.com/magazines/voyage/infos/dossiers/d/geographie-marais-mangrove-tannes-683/

Lima HV, Silva AP, Romero RE, Jacomine PKT (2005) Physical behavior of a gray cohesive Argisol in Ceara State. *Revista Brasileira de Ciencia do Solo* **29**, 33–40.

Lima HV, Silva AP, Santos MC, Cooper M, Romero RE (2006) Micromorphology and image analysis of a hardsetting Ultisol (Argissolo) in the State of Ceará (Brazil). *Geoderma* **132**, 416–426. doi:10.1016/j.geoderma.2005.06.006

Lobato FAO, de Andrade EM, Meireles ACM, Cristomo LA (2008) Seasonality of the irrigated water quality at the Distrito Irrigado Baixo Acaraú, Ceará, Brazil. *Revista Ciência Agronômica* **1**, 167–172.

Lord CJ III (1982) A selective and precise method for pyrite determination in sedimentary materials. *Journal of Sedimentary Petrology* **52**, 664–666. doi:10.1306/212F7FF4-2B24-11D7-8648000102C1865D

Maia LP, de Lacerda LD, Monteiro LHU, Souza GM (2006) 'Atlas dos manguezais do Nordeste do Brasil: avaliação das áreas de manguezais dos estados do Piauí, Ceará, Rio Grande do Norte, Paraíba e Pernambuco.' (SEMACE: Fortaleza, CE, Brazil)

Marchand C, Lallier-Vergès E, Allenbach M (2011) Redox conditions and heavy metals distribution in mangrove forests receiving effluents from shrimp farms (Teremba Bay, New Caledonia). *Journal of Soils and Sediments* **11**, 529–541. doi:10.1007/s11368-010-0330-3

Marius C (1985) 'Mangroves du Senegal et de la Gambie: ecologie-pédologie- géochimie, mise en valeur et aménagement.' (ORSTOM: Paris)

Marques AGB (2010) Characterization and genesis of mangrove, apicum salt flat and coastal tableland of Acaraú (Ceará State) coastal region. MSc Thesis, Universidade Federal do Ceará, Fortaleza, Ceará, Brazil.

Marques AGB, Ferreira TO, Cabral RL, Nóbrega GN, Romero RE, Meireles AJA, Otero XL (2013) Hypersaline tidal flats (Apicum Ecosystems): the weak link in the tropical wetland chains. *Environmental Reviews* **22**, 1–11. doi:10.1139/er-2013-0026

McBride MB (1994) 'Environmental chemistry of soil.' (Oxford University Press: New York)

Mehlich A (1953). 'Determination of P, Ca, Mg, K, Na, and NH_4.' STDP No. 1-53. (Soil Testing Division, Department of Agriculture: Raleigh, NC, USA)

Meireles AJA (2005) Riscos sócio-ambientais ao longo da zona costeira. Available at: http://www.sbpcnet.org.br/livro/57ra/programas/conf_simp/textos/antoniomeireles.htm

Meireles AJA, Raventos JS (2002) A integrated geomorphological model for the coastal plain of Jericoacoara/Ceará. *Mercator* **1**, 79–94.

Meireles AJA, Cassola RS, Tupinambá SV, Queiroz L de S (2007) Environmental impacts promoted by shrimp farm on the coast Ceará, northeastern Brazil. *Mercator* **6**, 83–106.

Meireles AJA, Silva EV, Thiers PRL (2010) Environmental impacts of the activities of shrimp farming in mangrove ecosystem of the Ceará State, Northeastern Brazil. *Revista da Gestão Costeira Integrada* **2**, 1–11.

Metson AJ (1956) 'Methods of chemical analysis for soil survey samples.' (New Zealand Soil Bureau: Wellington, New Zealand)

Munsell Color (2000) 'Munsell soil color chart.' (Munsell Color: Grand Rapids, MI, USA)

Nascimento S (1993) 'Estudo da importância do "apicum" para o ecossistema de manguezal. Relatório Técnico Preliminar.' (Governo do Estado do Sergipe: Aracaju, SE, Brazil)

Nóbrega GN, Ferreira TO, Romero RE, Marques AGB, Otero XL (2013) Iron and sulfur geochemistry in semi-arid mangrove soils (Ceará, Brazil) in relation to seasonal changes and shrimp farming effluents. *Environmental Monitoring and Assessment* **185**, 7393–7407. doi:10.1007/s10661-013-3108-4

Prada-Gamero RM, Vidal-Torrado P, Ferreira TO (2004) Mineralogy and physical chemistry of mangrove soils from Iriri River at the Bertioga Channel (Santos, São Paulo State, Brazil). *Revista Brasileira de Ciencia do Solo* **28**, 233–243. doi:10.1590/S0100-06832004000200002

Quaggio JA, van Raij B, Mallavolta E (1985) Alternative use of the SMP-buffer solution to determine lime requirement of soils. *Communications in Soil Science and Plant Analysis* **16**, 245–260. doi:10.1080/00103628509367600

Rhoades JD (1996) Salinity: Electrical conductivity and total dissolved solids. In 'Methods of soil analysis: Chemical methods. Part 3'. (Ed. DL Spark) (Soil Science Society of America: Madison, WI, USA)

Ridd PV, Stieglitz T (2002) Dry season salinity changes in arid estuaries fringed by mangroves and saltflats. *Estuarine, Coastal and Shelf Science* **54**, 1039–1049. doi:10.1006/ecss.2001.0876

Rogers K, Saintilan N, Cahoon D (2005) Surface elevation dynamics in a regenerating mangrove forest at Homebush Bay, Australia. *Wetlands Ecology and Management* **13**, 587–598. doi:10.1007/s11273-004-0003-3

Ruivo MLP, Amaral IG, Faro MPS, Ribeiro ELC, Guedes ALS, Santos MML (2005) Chemical characterization of the organic surface layer and light organic matter in different types of soil in a toposequence, in Algodoal Island, Maiandeua, Pará State, Boletim do Museu Paraense Emílio Goeldi. *Ciências Naturais* **1**, 227–234.

Sauermann G, Andrade JS Jr, Maia LP, Costa UMS, Araujo AD, Herrmann HJ (2003) Wind velocity and sand transport on a barchan dune. *Geomorphology* **54**, 245–255. doi:10.1016/S0169-555X(02)00359-8

Schaeffer-Novelli Y, Cintrón-Molero G, Soares ML, De-Rosa MMPT (2000) Brazilian mangroves. *Aquatic Ecosystem Health & Management* **3**, 561–570.

Schmidt AJ (2006) Estudo da dinâmica populacional do caranguejo-uçá, *Ucides cordatus cordatus* e dos efeitos de uma mortalidade em massa desta espécie em manguezais do Sul da Bahia. MSc Thesis, Universidade de São Paulo, São Paulo, SP, Brazil.

Schoeneberger PJ, Wysocki DA, Benham EC, Broderson WD (2002) 'Field book for describing and sampling soils, Version 2.0.' Natural Resources Conservation Service. (National Soil Survey Center: Lincoln, NE, USA)

Schwertmann U (1992) Relations between iron oxides, soil colors and soil formation. In ' Soil color'. pp. 51–70. (Soil Science Society of America: Madison, WI, USA)

Soil Survey Staff (2010) 'Keys to Soil Taxonomy.' 11th edn (United States Department of Agriculture, Natural Resources Conservation Service: Washington, DC)

Souza-Júnior VS, Vidal-Torrado P, Garcia-Gonzaléz MT, Otero XL, Macías F (2008) Soil mineralogy of mangrove forest from the state of São Paulo, Southeastern Brazil. *Soil Science Society of America Journal* **72**, 848–857. doi:10.2136/sssaj2007.0197

Stumm W, Morgan JJ (1996) 'Aquatic Chemistry. Chemical equilibria and rates in natural waters.' (Wiley Interscience: New York)

Sucupira PAP, Pinheiro L de S, Rosa M de S (2006) Caracterização morfométrica do médio e baixo curso do rio Acaraú-Ceará-Brasil. Regional Conference on Geomorphology, Goiânia, GO, Brazil. Available at: http://www.labogef.iesa.ufg.br/links/sinageo/articles/059.pdf

Suguio K, Martin L, Bittencourt ACSP, Dominguez JML, Flexor JM, Azevedo AEG (1985) Flutuações do nível relativo do mar durante o Quaternário Superior ao longo do litoral brasileiro e suas implicações na sedimentação costeira. *Revista Brasileira de Geociencias* **15**, 273–286.

Sullivan LA, Fitzpatrick RW, Bush RT, Burton ED, Shand P, Ward NJ (2010). 'The classification of acid sulfate soil materials: further modifications.' Southern Cross GeoScience Technical Report. (Southern Cross University: Lismore, NSW, Australia)

Sumner ME, Miller WP (1996) Cation exchange capacity and exchange coefficients. In 'Methods of soil analysis, Part 3'. (Chemical methods. Soil Science Society of America: Madison, WI, USA)

Torrentó C, Cama J, Urmeneta J, Otero N, Soler A (2010) Denitrification of groundwater with pyrite and *Thiobacillus denitrificans. Chemical Geology* **278**, 80–91. doi:10.1016/j.chemgeo.2010.09.003

Ucha JM, Hadlich GM, Celino JJ (2008) Apicum: transição entre solos de encosta e manguezais. *Revista Educação Tecnologia e Cultura* **5**, 58–63.

van Breeman N, Buurman P (2002) 'Soil formation.' 2nd edn.(Kluwer: New York)

Velde B, Church T (1999) Rapid clay transformations in Delaware salt marshes. *Applied Geochemistry* **14**, 559–568. doi:10.1016/S0883-2927(98)00092-4

Vermeulen J, Grotenhuis T, Joziasse J, Rulkens W (2003) Ripening of dredged sediments during temporary upland disposal. A bioremediation technique. *Journal of Soils and Sediments* **3**, 49–59. doi:10.1007/BF02989469

Vieillefon J (1969) 'La pédogénèse dans les mangroves tropicales. Un exemple de chronoséquence.' (ORSTOM: Paris)

Vieira JM, Romero RE, Ferreira TO, Assis Júnior RNA (2012) Contribution of amorphous material in the genesis of cohesive horizons of Ultisols in

Ceara Coastal Plains. *Revista Ciência Agronômica* **43**, 623–632. doi:10.1590/S1806-66902012000400002

Vilhena MDP, Costa MLD, Berrêdo JF (2010) Continental and marine contributions to formation of mangrove sediments in an eastern Amazonian mudplain: the case of the Marapanim Estuary. *Journal of South American Earth Sciences* **29**, 427–438. doi:10.1016/j.jsames.2009.07.005

Zack A, Román-Mas A (1988) Hydrology of the Caribbean Island Wetlands. *Acta Científica* **2**, 65–73.

Zenova GM, Oborotov GV, Norovsuren ZH, Fedotova AV, Yakovleva LV (2007) Halophilic and Alkaliphilic Streptomycetes in Salt-Affected Soils. *Eurasain Soil Science* **40**, 1203–1207. doi:10.1134/S1064229307110087